A Journal of the Gesellschaft Deutscher Chemiker

Angewandte Chemie

GDCh

International Edition

www.angewandte.org

Accepted Article

Title: Dirhodium-Catalyzed Enantioselective B–H Bond Insertion of gem-Diaryl Carbenes: Efficient Access to gem-Diarylmethine Boranes

Authors: Yu-Tao Zhao, Yu-Xuan Su, Xiao-Yu Li, Liang-Liang Yang, Ming-Yao Huang, and Shou-Fei Zhu

To be cited as: *Angew. Chem. Int. Ed.* 10.1002/anie.202109447

Link to VoR: https://doi.org/10.1002/anie.202109447

WILEY-VCH

10.1002/anie.202109447

WILEY-VCH

RESEARCH ARTICLE

Dirhodium-Catalyzed Enantioselective B–H Bond Insertion of *gem*-Diaryl Carbenes: Efficient Access to *gem*-Diarylmethine Boranes

Yu-Tao Zhao,[a] Yu-Xuan Su,[a] Xiao-Yu Li,[a] Liang-Liang Yang,[a] Ming-Yao Huang,[a] Shou-Fei Zhu*[a]

Dedicated to 100th Anniversary of Chemistry at Nankai University.

[a] Y.-T. Zhao, Y.-X. Su, X.-Y. Li, L.-L Yang, M.-Y. Huang, Prof. Dr. S.-F. Zhu
Frontiers Science Center for New Organic Matter, State Key Laboratory and Institute of Elemento-Organic Chemistry, College of Chemistry, Nankai University, Tianjin 300071, China
E-mail: sfzhu@nankai.edu.cn

Supporting information for this article is given via a link at the end of the document

Abstract: Chiral *gem*-diarylmethine boron compounds are important synthetic building blocks that can be transformed into chiral *gem*-diaryl methanes or triaryl methanes, which are common scaffolds in bioactive molecules. However, the scarcity of reliable methods for synthesizing chiral *gem*-diarylmethine borons limits their applications. Herein, we report a method for highly enantioselective dirhodium-catalyzed B–H bond insertion reactions with diaryl diazomethanes as carbene precursors. These reactions afforded chiral *gem*-diarylmethine borane compounds in high yield (up to 99% yield), high activity (turnover numbers up to 14,300), high enantioselectivity (up to 99% ee) and showed unprecedented broad functional group tolerance. Moreover, the borane compounds synthesized by this method could be efficiently transformed into diaryl methanol, diaryl methyl amine, and triaryl methane derivatives with good stereospecificity. Mechanistic studies suggested that the borane adduct coordinated to the rhodium catalyst and thus interfered with decomposition of the diazomethane, and that insertion of a rhodium carbene (generated from the diaryl diazomethane) into the B–H bond was most likely the rate-determining step. Hammett analysis indicated that the enantioselectivity depended strongly on electronic differences between the two aryl groups of the diazomethane.

Introduction

Organoboron compounds are widely used in organic synthesis, materials science, medicine, and other fields.[1–9] In particular, chiral *gem*-diarylmethine boron compounds, which have a unique *gem*-diaryl framework, are powerful tools for the construction of bioactive compounds with a diaryl methane[10–12] or triaryl methane[12–16] motif *via* C–B bond transformations. Therefore, enantioselective synthesis of *gem*-diarylmethine boron compounds has attracted widespread interest, but it nevertheless remains a challenge. Since 2008, Aggarwal and coworkers[17–19] have published several reports on lithiation-borylation reactions of chiral benzyl carbamates with aryl boronates for asymmetric synthesis of *gem*-diarylmethine borates containing a chiral quaternary carbon center (Scheme 1A). Crudden and coworkers[20] modified Aggarwal's protocol by adding an equivalent of chiral bisoxazoline ligands to prepare *gem*-diarylmethine boronic esters with a chiral tertiary carbon center, and these investigators used their protocol to synthesize

Scheme 1. Methods for synthesis of chiral *gem*-diarylmethine boron compounds

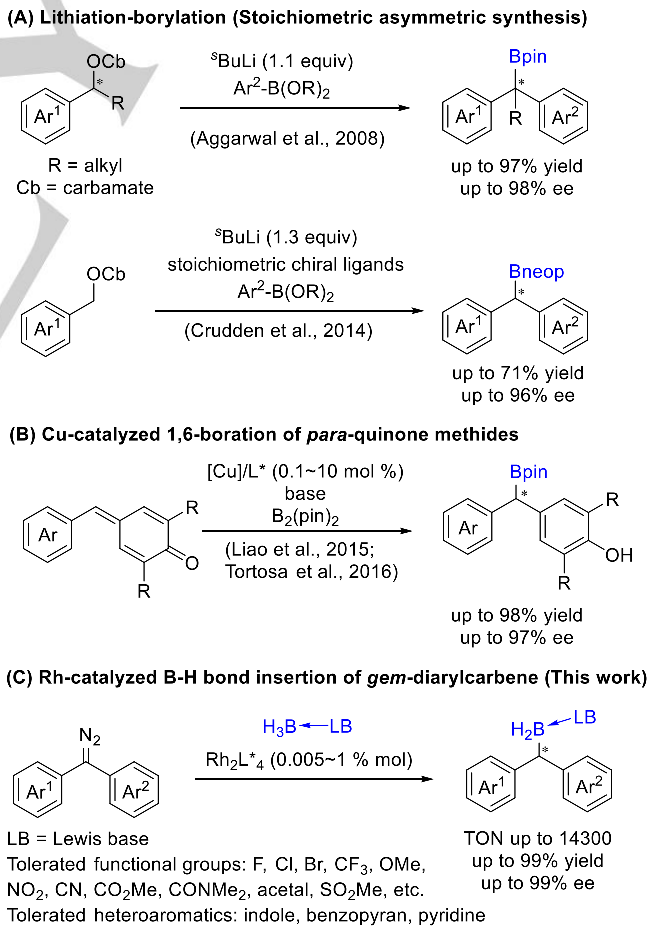

chiral triaryl methane derivatives (Scheme 1A). Recently, the groups of Liao [21] and Tortosa[22] independently developed copper-

10.1002/anie.202109447

catalyzed 1,6-boration reactions of *para*-quinone methides for construction of chiral *gem*-diarylmethine borates (Scheme 1B). To the best of our knowledge, this is the only catalytic asymmetric method for accessing *gem*-diarylmethine boron compounds. The use of strong bases in all the above-mentioned methods strongly limits the functional group diversity of the *gem*-diarylmethine boron products. For instance, commonly encountered functionality such as esters, nitro groups, nitriles, and amides are incompatible with these methods. Moreover, for 1,6-boration of *para*-quinone methides (Scheme 1B), the steric requirements for the substrates substantially limit the structural diversity of the products.

We reasoned that B–H bond insertion reactions of carbenes might be useful for the synthesis of *gem*-diarylmethine boranes. Transition-metal-catalyzed asymmetric B–H bond insertion reactions of carbenes have provided a new method for the synthesis of chiral organoboron compounds.[23–32] Since we reported the first example of a copper-catalyzed asymmetric B–H bond insertion reaction with α-diazophenylacetate as a carbene precursor,[25] catalytic asymmetric B–H bond insertion reactions have been successfully used for enantioselective construction of B–C bonds. Various carbene precursors such as α-diazophenylacetates,[25,27,33] α-diazophenylketones,[26,27] α-diazopropionates,[30,32] trifluorodiazoalkanes,[28] ene-yne-carbonyls,[29] and tosylhydrazones[31] have been used in these insertion reactions. Although with these progresses, the catalytic enantioselective B–H bond insertion still in its infancy comparing with the close related well-established catalytic enantioselective C–H bond insertion.[34–37] Thus, the use of B–H bond insertion in the synthesis of inconveniently available chiral organoboron compounds is highly desired. Herein, we report an efficient method for the synthesis of chiral *gem*-diarylmethine boron compounds by means of B–H bond insertion reactions of diaryl diazomethane compounds with catalysis by commercially available chiral dirhodium complexes (Scheme 1C). Compared with the known methods for synthesis of *gem*-diarylmethine boron compounds, our method showed greatly enhanced functional group tolerance and thus enabled highly enantioselective synthesis of chiral *gem*-diarylmethine boron compounds with unprecedented structural diversity. Moreover, the compounds prepared in this study were bench-stable and could undergo several important functional group transformations with high preservation of stereochemistry, exhibiting great application prospects.

Results and Discussion

The highly enantioselective rhodium-catalyzed Si–H bond insertion reactions[38,39] and cyclopropanation reactions[40] using diaryl carbenes have been well established recently. Inspired by these pioneer works, we began our studies by carrying out reactions of 4-nitrophenyl phenyl diazomethane (**1a**) with trimethylamine-borane adduct **2a** in the presence of 1 mol % of various chiral dirhodium catalysts in DCM at room temperature (Table 1). The B–H bond insertions were complete in minutes, giving desired *gem*-diarylmethine borane **3aa** in moderate to high yields (entries 1–9). Of the tested catalysts, Rh_2(*S*-TBPTTL)$_4$ gave the highest yield and enantioselectivity (entry 4). Solvent screening revealed that other chlorinated solvents gave similar outcomes (compare entries 4, 10, and 11); whereas a coordinative solvent (THF) markedly decreased the reaction rate (entry 12), and a nonpolar solvent (toluene) slightly improved the enantioselectivity and the yield (entry 13). Lowering the reaction temperature improved the enantioselectivity further without compromising the yield (entries 13–16): **3aa** was obtained in 96% yield and 91% ee at −40 °C in toluene (entry 16). We also tested numbers of chiral Cu(I) and Rh(I) catalysts in the template reaction but got unsatisfactory results (see Table S1 and Table S2 for details).

Table 1. Rh-catalyzed enantioselective B−H bond insertion of 4-nitrophenylphenyl diazomethane **1a** with trimethylamine-borane adduct **2a**: optimization of reaction conditions[a]

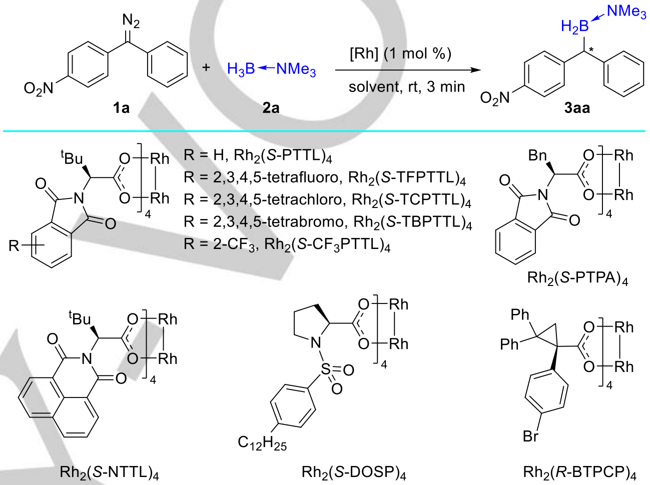

entry	[Rh]	solvent	Yield (%)	ee (%)
1	Rh_2(*S*-PTTL)$_4$	DCM	92	-9
2	Rh_2(*S*-TFPTTL)$_4$	DCM	76	64
3	Rh_2(*S*-TCPTTL)$_4$	DCM	89	81
4	Rh_2(*S*-TBPTTL)$_4$	DCM	91	83
5	Rh_2(*S*-CF_3PTTL)$_4$	DCM	88	17
6	Rh_2(*S*-PTPA)$_4$	DCM	91	0
7	Rh_2(*S*-NTTL)$_4$	DCM	83	16
8	Rh_2(*S*-DOSP)$_4$	DCM	63	14
9	Rh_2(*R*-BTPCP)$_4$	DCM	55	11
10	Rh_2(*S*-TBPTTL)$_4$	DCE	95	80
11	Rh_2(*S*-TBPTTL)$_4$	PhCl	96	88
12[b]	Rh_2(*S*-TBPTTL)$_4$	THF	85	89
13	Rh_2(*S*-TBPTTL)$_4$	PhMe	97	86
14[c]	Rh_2(*S*-TBPTTL)$_4$	PhMe	94	88
15[d]	Rh_2(*S*-TBPTTL)$_4$	PhMe	95	89
16[b],[e]	Rh_2(*S*-TBPTTL)$_4$	PhMe	96	91

[a] Reaction conditions (procedure A): [Rh]/**1a**/**2a** = 0.002:0.2:0.24 (mmol), 2 mL solution of **1a** was dropped into a 2 mL solution of **2a** and [Rh]. All the reactions were completed within 3 min unless otherwise noted. Isolated yields were given. The ee values were determined by chiral HPLC, using chiral IC-3 column. [b] Reaction time: 10 min. [c] Performed at 0 °C. 10 min. [d] Performed at -20 °C. [e] Performed at -40 °C.

10.1002/anie.202109447

A series of borane adducts **2** were then evaluated in reactions with diazomethane **1a** (Table 2). Tertiary amine- and phosphine-borane adducts smoothly underwent B–H bond insertion reactions and afforded the desired products in high yields with ee values similar to those obtained with **2a** (entries 1–5, 8, 9), whereas a borane adduct stabilized by a secondary amine failed to give any of the desired product due to catalyst decomposition (entry 6). 3,5-Dimethylpyridine-borane **2f** and N-heterocyclic carbene-borane **2i** also afforded high yields with moderate enantioselectivities under the standard reaction conditions (entries 7 and 10).

Table 2. Rh-catalyzed asymmetric B–H bond insertion of 4-nitrophenylphenyl diazomethane **1a** with various borane adducts[a]

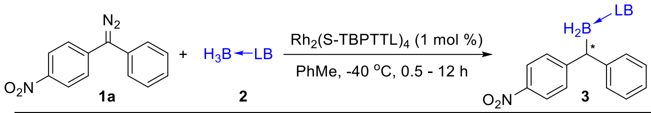

entry	LB	product	yield (%)	ee (%)
1	NMe_3	**3aa**	96	91
2	NEt_3	**3ab**	99	90
3	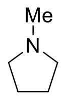	**3ac**	95	92
4	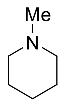	**3ad**	97	91
5	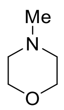	**3ae**	80	90
6	$NHMe_2$	NA	NA	NA
7	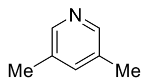	**3af**	95	76
8	P^nBu_3	**3ag**	82	92
9	PMe_2Ph	**3ah**	92	86
10	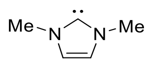	**3ai**	84	71

[a] Reaction conditions: Rh_2(*S*-TBPTTL)$_4$/**1a**/**2** = 0.002/0.2/0.24 (mmol), 2 mL solution of **1a** was dropped into a 2 mL solution of **2a** and Rh_2(*S*-TBPTTL)$_4$. Isolated yields were given. The ee values were determined by chiral HPLC. NA = Not available.

Next, we investigated Rh_2(*S*-TBPTTL)$_4$-catalyzed asymmetric B–H bond insertion reactions of various diaryl diazomethanes **1** with amine-borane adduct **2a** (Scheme 2). The reactions of all the tested diazo substrates smoothly gave the desired *gem*-diarylmethine borane compounds in good to excellent yields with high enantioselectivities (71–99% ee). Various functional groups, including nitro groups (**3aa**–**3la**), halogen atoms (**3fa**–**3ha**), trifluoromethyl groups (**3ia**, **3ta**), an acetal (**3la**), an amide (**3ma**), an ester (**3na**), a sulfone (**3oa**), a trifluoromethoxy group (**3pa**), and a cyano group (**3qa**), were well tolerated under the reaction conditions. The enantioselectivity appeared to depend on electronic differences between the Ar^1 and Ar^2 groups of diaryl diazomethane substrates **1**, where the electron donor and acceptor groups on each aryl ring play an important role. This phenomenon was consistent with previous studies.[38–40] When Ar^1 had an electron-withdrawing *para*-nitro group, the enantioselectivity decreased as the electron-donating ability of the substituent on Ar^2 decreased (**3aa**–**3ia**). Substrates with an

Scheme 2. Rh-catalyzed asymmetric B–H bond Insertion of diarylcarbenes: substrate scope[a]

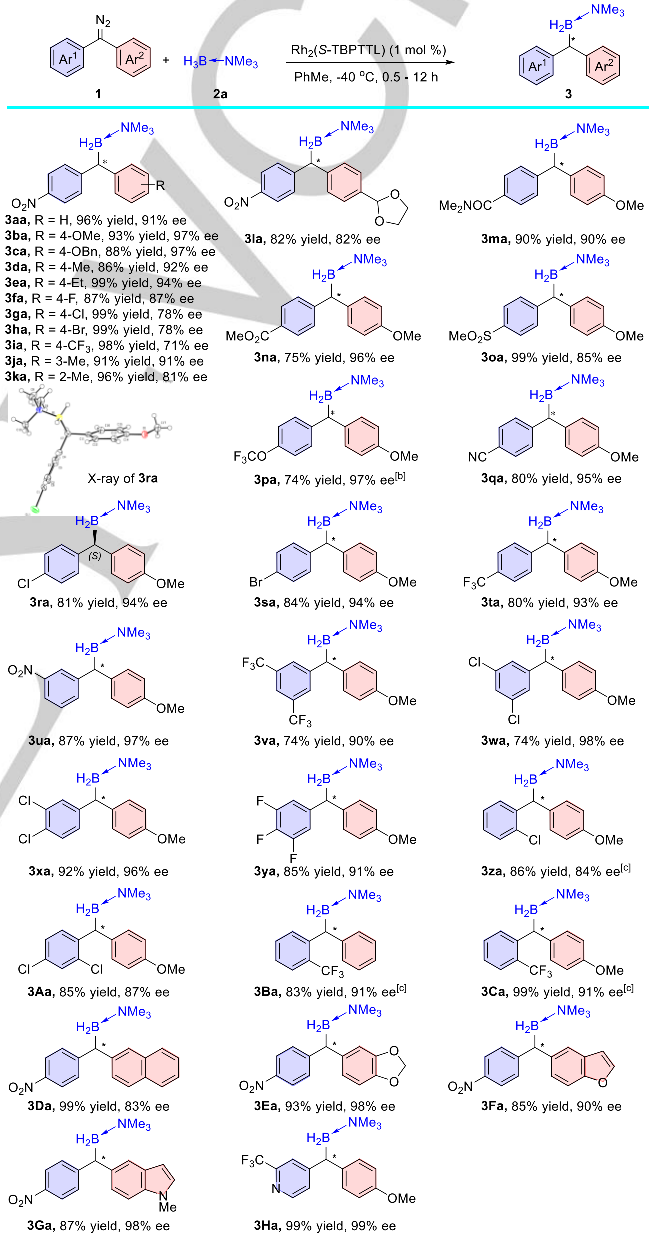

[a] Reaction conditions (procedure A): Rh_2(S-TBPTTL)$_4$/**1**/**2a** = 0.002/0.2/0.24 (mmol), PhMe, -40 °C, 0.5–12 h. Isolated yields were given. The ee values were determined by chiral HPLC analysis. For substrate **1A**, the reaction was performed at 0 °C. [b] Reaction conditions (procedure B): hydrazone (0.2 mmol), activated MnO_2 (1 mmol), $MgSO_4$ (0.24 mmol), DCM, 0 °C, 2–3 h; then **2a** (0.24 mmol), Rh_2(*S*-TBPTTL)$_4$ (0.002 mmol), PhMe, -40 °C, 6 h. [c] Reaction conditions (procedure C): hydrazone (0.2 mmol), activated MnO_2 (1 mmol), $MgSO_4$ (0.24 mmol), DCM, 0 °C, 2 – 3 h; then **2a** (0.24 mmol), Rh_2(*S*-TBPTTL)$_4$ (0.002 mmol), PhMe, 0 °C, 6 h.

10.1002/anie.202109447

ortho- or *meta*-substituted Ar^2 ring also showed fairly good enantioselectivities (**3ja**, **3ka**). We also investigated how substituents on Ar^1 affected the enantioselectivity when Ar^2 had an electron-donating *para*-methoxy group (**3ma**–**3Aa**, **3Ca**). Most of the B–H bond insertion products were obtained with ee values higher than 90%. We noticed that the enantioselectivity was enhanced by increasing the electron-withdrawing ability of the substituent on Ar^1 (**3ma**–**3ua**). The structures and absolute configurations of **3ba** and **3ra** were determined by X-ray diffraction analysis of single crystals.[41] Interestingly, when Ar^1 had an *ortho* substituent, the enantioselectivity was only slightly affected by the other substituents on Ar^1 or Ar^2 (**3za**–**3Ca**). Diazo substrates containing other aryl groups, including naphthyl (**3Da**), piperonyl (**3Ea**), benzofuryl (**3Fa**), indolyl (**3Ga**), and pyridinyl (**3Ha**), also exhibited excellent enantioselectivity. Notably, all the B–H bond insertion products were stable during purification operations (e.g., chromatography and recrystallization) and could be stored for several months without any decomposition. The high stability of the products may be attributable to their coordinatively saturated boryl groups.

Scheme 3. Gram-scale experiments and transformations of product **3ra**

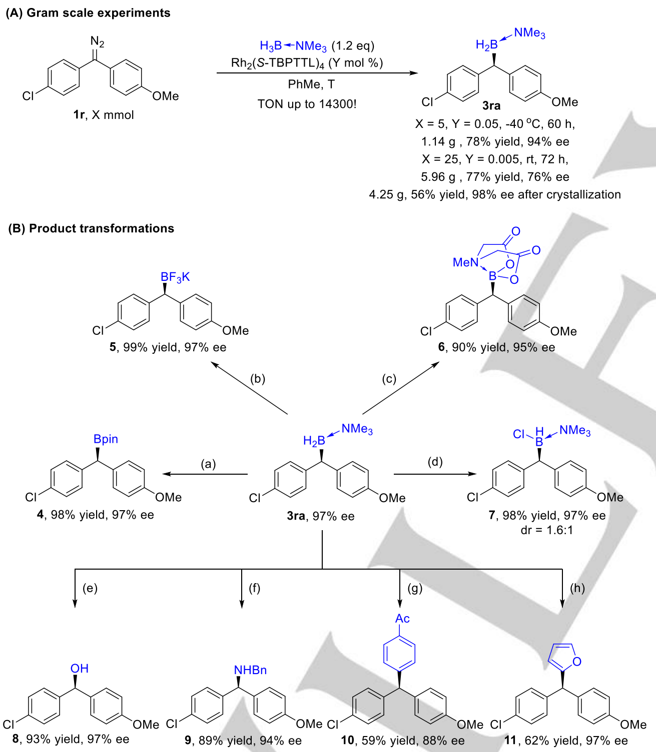

Reaction conditions: (a) pinacol, PhMe, 90 °C, 1h; (b) KHF_2 (aq.), dioxane, reflux, 2 h; (c) *N*-methyl imidodiacetic acid, toluene/DMSO = 5:1, 110 °C, 17 h; (d) *N*-chlorosuccinimide, THF, 1 h; (e) H_2O_2, MeOH, reflux, 17 h; (f) KHF_2 (aq.), dioxane, reflux, 2 h; then $SiCl_4$, DCE, 0 °C – rt, 1 h; then BnN_3, DCE, 80 °C, 1 h; then NaOH (aq.); (g) 2,2-dimethyl-1,3-propanediol, PhMe, 100 °C, 2 h; then, 4-iodoacetophenone, $Pd(PPh_3)_4$, Ag_2O, K_2CO_3, Et_2O, 60 °C, 17 h; (h) pinacol, PhMe, 100 °C, 1 h; then 2-lithiofuran, -78 °C, 1 h; then *N*-bromosuccinimide, -78 °C, 1 h.

The synthetic potential of this B–H bond insertion reaction was then examined (Scheme 3). The reaction could be conducted at a gram scale with a catalyst loading of 0.05 mol % without compromising either the yield or the enantioselectivity, and the ee value of B–H bond insertion product (*S*)-**3sa** could be improved by crystallization (Scheme 3A). The turnover number reached 14,300, which, to our knowledge, is the highest turnover number reported for a B–H bond insertion reaction promoted by a molecular catalyst.[23–33,42–48] In addition, borane (*S*)-**3sa** could easily be converted into widely used boron reagents: chiral boronic ester **4**, potassium trifluoroborate **5**, and MIDA (methyliminodiacetic acid) borate **6** (Scheme 3B). Interestingly, we accidentally discovered that reaction of (*S*)-**3sa** with *N*-chlorosuccinimide resulted in a nearly quantitative yield of unprecedented chlorinated boron **7**. In addition, (*S*)-**3sa** could be transformed to alcohol **8** by oxidation with H_2O_2, to dibenzylic amine **9** *via* a potassium trifluoroborate intermediate in one pot,[49] and to chiral triaryl methanes **10** and **11** by means of sp^2–sp^3 coupling reactions.[18,20] In most cases, the stereochemistry was well retained during the transformations as described in the literatures,[18,20,49] showing the potential utility of this protocol.

Scheme 4. Control experiments

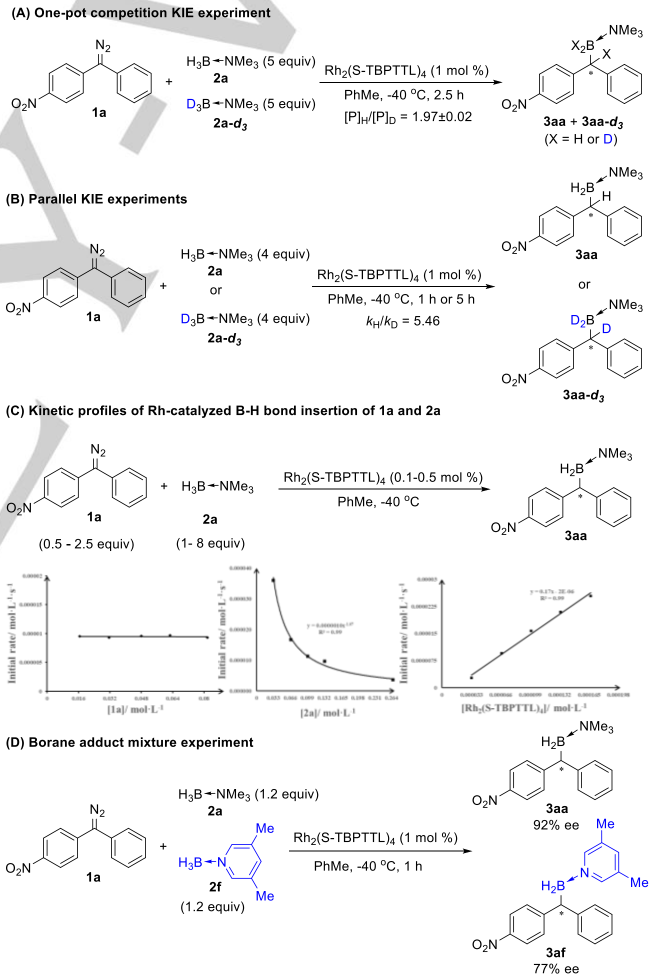

To elucidate the reaction mechanism, we carried out both a competitive kinetic isotope effect (KIE) experiment (k_H/k_D = 1.97) and a parallel KIE experiment (k_H/k_D = 5.46) involving the reaction between **1a** and **2a** (Scheme 4A and 4B, respectively). The large, primary KIE indicates that B–H bond cleavage might be involved in the rate-limiting step. To gain deeper insight into the mechanism, we determined the reaction order of every component by using in situ IR to measure the initial reaction rate

10.1002/anie.202109447

at a series of concentrations of each component (Scheme 4C). These experiments indicated that the kinetics were first order for the Rh_2(*S*-TBPTTL)$_4$ catalyst, zero order for diazomethane **1a**, and negative first order for borane adduct **2a**. The kinetics profiles suggest that decomposition of **1a** is not the rate-determining step and that **2a** might inhibit decomposition of **1a** by binding to the active site of the dirhodium catalyst.[50] The interaction of the borane adduct with the dirhodium catalyst was confirmed by the fact that changes in the UV spectra of Rh_2(*S*-TBPTTL)$_4$ in toluene were observed upon addition of **2a** (Fig. S1). The pre-equilibrium formation of a resting-state complex of Rh_2(*S*-TBPLL)$_4$ and **2a** might contribute to the striking difference between the competitive and parallel k_H/k_D values. Reactions of a mixture of borane adducts in one pot gave enantioselectivities similar to those obtained for reactions in separate pots, suggesting that only one molecule of the borane adduct is involved in the enantio-determining step (Scheme 4D).

Scheme 5. Calculated catalytic cycle,[a] chiral control model,[b] and Hammett plots[c]

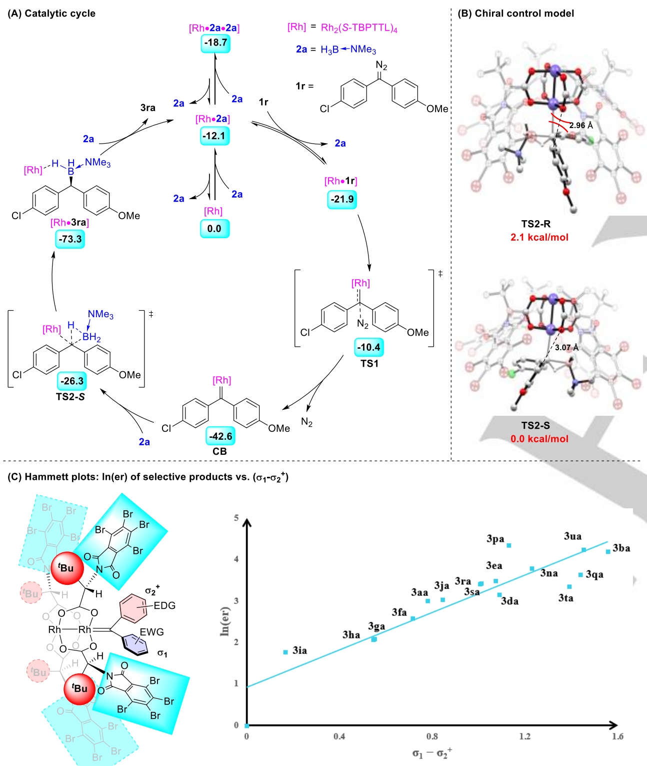

[a] Calculated catalytic cycle of rhodium-catalyzed B–H insertion of **1r** and **2a**. Density functional theory calculations were performed at the B3LYP-D3(BJ)/DEF2TZVP/SMD(PhMe)//B3LYP/DEF2SVP. Gibbs free energies relative to **[Rh]** were given in the bright blue box. [b] Optimized lowest-energy transition structures for *R* and *S* products. Gibbs free energies were given relative to **TS2-S**. [c] Hammett studies. Hammett parameters σ and σ$^+$ were used for electron-withdrawing group (EWG-) and electron-donating group (EDG-) substituted arenes, respectively. Other correlation trials were given in Tables S3–S5 in the Supporting Information.

In addition, we conducted density functional theory calculations (Gaussian 09) on the rhodium-catalyzed reaction of diazomethane **1r** and amine-borane adduct **2a** (Scheme 5A). The calculations indicate that the catalytic cycle starts with dissociation of one borane adduct from [Rh•**2a**•**2a**] (a process that is uphill by 6.6 kcal/mol). Diazomethane **1r** coordinates to the rhodium catalyst by replacing **2a** and then decomposes to release N_2 and carbene intermediate **CB** *via* transition state **TS1**, a process with an activation energy of only 11.5 kcal/mol. Once formed, **CB** can insert into the B–H bond of **2a** *via* three-membered-ring transition state **TS2-S**, generating the desired product and releasing the catalyst to start another catalytic cycle. The B–H bond insertion process has an activation energy of 16.3 kcal/mol, which is 4.8 kcal/mol higher than the energy for diazo decomposition. These results indicate that B–H insertion is the rate-determining step, which agrees well with the results of the KIE experiments and with the zero order kinetics observed for diazomethane **1a** (Scheme 4A–4C). The irreversible B–H bond insertion can be considered as the enantio-determining step. The structures corresponding to the lowest-energy transition states for the major and minor enantiomers of the product are presented in Scheme 5B. In these two transition states **TS2-R** and **TS2-S**, the p-OMe aryl ring tends to adopt a more coplanar orientation with carbene p orbital, while p-Cl aryl ring adopts a tilted conformation. Such orientation difference of two aryl rings causes steric difference in asymmetrical environment of catalyst. [38–40] In accord with experimental observations, the calculated energy of **TS2-S** was 2.1 kcal/mol lower than that of **TS2-R**, which leads to the disfavored enantiomer, (*R*)-**3ra**. This energy difference might arise from steric repulsion between the *p*-OMe-substituted arene and the carboxylate group of the rhodium catalyst in **TS2-R**, repulsion that is absent in **TS2-S**.

Hammett analysis established that the enantioselectivity, ln(er), was linearly related to the electronic difference ($\sigma_1 - \sigma_2^+$) between the two arene rings of the diazo substrates (Scheme 5C). This result is consistent with the buildup of positive charge on the carbene carbon after decomposition of the diazomethane. The positive charge buildup causes the different behavior of the two aryl rings: the electron-deficient ring tends to be tilted out of the plane of the rhodium carbene, whereas the electron-rich ring tends to be coplanar with the carbene.[38,40,51] The greater the electronic difference between the two arenes is, the better the enantioselectivity will be.

Conclusion

In summary, we have realized a method for rhodium-catalyzed chiral B–H bond insertion reactions of borane adducts and diaryl diazomethanes. Using this method, we prepared various *gem*-diarylmethine borane compounds in high yield with excellent enantioselectivity, and the mild reaction conditions showed good functional group tolerance. The B–H insertion products could easily be transformed to widely used pinacolborates, potassium trifluoroborates, MIDA borates, diaryl methanol compounds, diaryl methyl amines, and triaryl methanes. Kinetics experiments and density functional theory calculations suggest that the borane adduct coordinates to the rhodium catalyst and interferes with decomposition of the diazomethane and that insertion of the rhodium carbene into the B–H bond is the rate-determining step (rather than diazomethane decomposition). Hammett plots showed that the enantioselectivity of the reaction correlates to electronic differences between the two aryl groups of the diazomethane. This method not only opens up a new route to *gem*-diarylmethine boranes but also deepens our understanding of B–H bond insertion reactions.

Acknowledgements

We thank National Natural Science Foundation of China (21625204 and 21971119), the "111" project (B06005) of the Ministry of Education of China, National Program for Support of Top-notch Young Professionals, Key-Area Research Development Program of Guangdong Province (2020B010188001), and Frontiers Science Center for New Organic Matter at Nankai University (63181206) for financial support. We also thank Prof. Mark D. Levin of the University of Chicago for helpful discussion on reaction mechanism and thank Prof. Xiao-Chen Wang of Nankai University for generously providing the chiral diene ligand **L11**.

Keywords: *gem*-diarylmethine boranes • B−H bond insertion • diaryl carbenes • diaryl diazomethanes • chiral dirhodium catalysts

[1] D. G. Hall, Boronic Acids: Preparation and Applications in Organic Synthesis, Medicine and Materials, 2nd ed.; Wiley-VCH: Weinheim, 2012.
[2] N. Miyaura, A. Suzuki, *Chem. Rev.* **1995**, *95*, 2457–2483.
[3] H. Braunschweig, R. D. Dewhurst, A. Schneider, *Chem. Rev.* **2010**, *110*, 3924–3957.
[4] V. M. Dembitsky, A. A. A. A. Quntar, M. Srebnik, *Chem. Rev.* **2011**, *111*, 209–237.
[5] D. Leonori, V. K. Aggarwal, *Angew. Chem. Int. Ed.* **2015**, *54*, 1082–1096; *Angew. Chem.* **2015**, *127*, 1096–1111.
[6] W. L. A. Brooks, B. S. Sumerlin, *Chem. Rev.* **2016**, *116*, 1375–1397.
[7] S. Namirembe, J. P. Morken, *Chem. Soc. Rev.* **2019**, *48*, 3464–3474.
[8] S.-Y. Liu, D. W. Stephen, *Chem. Soc. Rev.* **2019**, *48*, 3434–3435.
[9] M. Wang, Z. Shi, *Chem. Rev.* **2020**, *120*, 7348–7398.
[10] A. L. McRae, K. T. Brady, *Expert Opin. Pharmacother.* **2001**, *2*, 883–892.
[11] C. J. Hills, S. A. Winter, J. A. Balfour, *Drugs* **1998**, *55*, 813–820.
[12] S. Mondal, G. Panda, *RSC Adv.* **2014**, *4*, 28317–28358.
[13] S. B. Bodendiek, C. Rubinos, M. P. Trelles, N. Coleman, D. P. Jenkins, H. Wulff, M. Srinivas, *Front. Pharmacol.* **2012**, *3*, 1–17.
[14] M. S. Shchepinov, V. A. Korshun, *Chem. Soc. Rev.* **2003**, *32*, 170–180.
[15] V. Nair, S. Thomas, S. C. Mathew, K. G. Abhilash, *Tetrahedron* **2006**, *62*, 6731–6747.
[16] R. Palchaudhuri, V. Nesterenko, P. J. Hergenrother, *J. Am. Chem. Soc.* **2008**, *130*, 10274–10281.
[17] J. L. Stymiest, V. Bagutski, R. M. French, V. K. Aggarwal, *Nature* **2008**, *456*, 778–783.
[18] A. Bonet, M. Odachowski, D. Leonori, S. Essafi, V. K. Aggarwal, *Nat. Chem.* **2014**, *6*, 584–589.
[19] S. Roesner, J. M. Casatejada, T. G. Elford, R. P. Sonawane, V. K. Aggarwal, *Org. Lett.* **2011**, *13*, 5740–5743.
[20] S. C. Matthew, B. W. Glasspoole, P. Eisenberger, C. M. Crudden, *J. Am. Chem. Soc.* **2014**, *136*, 5828–5831.
[21] Y. Lou, P. Cao, T. Jia, Y. Zhang, M. Wang, J. Liao, *Angew. Chem. Int. Ed.* **2015**, *54*, 12134–12138; *Angew. Chem.* **2015**, *127*, 12302–12306.
[22] C. Jarava-Barrera, A. Parra, A. López, F. Cruz-Acosta, D. Collado-Sanz, D. J. Cárdenas, M. Tortosa, *ACS Catal.* **2016**, *6*, 442–446.
[23] J.-M. Yang, Z.-Q. Li, S.-F. Zhu, *Chin. J. Org. Chem.* **2017**, *37*, 2481–2497.
[24] M.-Y. Huang, S.-F. Zhu, *Chem. J. Chin. Univ.* **2020**, *41*, 1426–1448.
[25] Q.-Q. Cheng, S.-F. Zhu, Y.-Z. Zhang, X.-L. Xie, Q.-L. Zhou, *J. Am. Chem. Soc.* **2013**, *135*, 14094–14097.
[26] Q.-Q. Cheng, H. Xu, S.-F. Zhu, Q.-L. Zhou, *Acta Chim. Sinica* **2015**, *73*, 326–329.
[27] D. Chen, X. Zhang, W.-Y. Qi, B. Xu, M.-H. Xu, *J. Am. Chem. Soc.* **2015**, *137*, 5268–5271.
[28] S. Hyde, J. Veliks, B. Liégault, D. Grassi, M. Taillefer, V. Gouverneur, *Angew. Chem. Int. Ed.* **2016**, *55*, 3785–3789; *Angew. Chem.* **2016**, *128*, 3849 –3853.
[29] J.-M. Yang, Z.-Q. Li, M.-L. Li, Q. He, S.-F. Zhu, Q.-L. Zhou, *J. Am. Chem. Soc.* **2017**, *139*, 3784–3789.
[30] S. B. J. Kan, X. Huang, Y. Gumulya, K. Chen, F. H. Arnold, *Nature* **2017**, *552*, 132–136.
[31] Y. Pang, Q. He, Z.-Q. Li, J.-M. Yang, J.-H. Yu, S.-F. Zhu, Q.-L. Zhou, *J. Am. Chem. Soc.* **2018**, *140*, 10663–10668.
[32] N. Otog, S. Chanthamath, I. Fujisawa, S. Iwasa, *Eur. J. Org. Chem.* **2021**, 1564–1567.
[33] N. M. Ankudinov, D. A. Chusov, Y.V. Nelyubina, D. S. Perekalin, *Angew. Chem. Int. Ed.* **2021**, *60* DOI:10.1002/anie.202105179; *Angew. Chem.* **2021**, *133*, DOI:10.1002/anie.202105179.
[34] H. M. L. Davies, J. R. Manning, *Nature*, **2008**, *451*, 417–424.
[35] M. P. Doyle, R. Duffy, M. Ratnikov, L. Zhou, *Chem. Rev.* **2010**, *110*, 704–724.
[36] H. M. L. Davies, D. Morton, *Chem. Soc. Rev.*, **2011**, *40*, 1857–1869.
[37] H. M. L. Davies, K. Liao, *Nature Rev. Chem.* **2019**, *3*, 347–360.
[38] L.-L. Yang, D. Evans, B. Xu, W.-T. Li, M.-L. Li, S.-F. Zhu, K. N. Houk, Q.-L. Zhou, *J. Am. Chem. Soc*. **2020**, *142*, 12394–12399.
[39] J. R. Jagannathan, J. C. Fettinger, J. T. Shaw, A. K. Franz, *J. Am. Chem. Soc.* **2020**, *142*, 11674−11679.
[40] M. Lee, Z. Ren, D. G. Musaev, H. M. L. Davies, *ACS Catal.* **2020**, *10*, 6240–6247.
[41] CCDC 2081551 and 2081552 contain the supplementary crystallographic data for this paper. The data can be obtained free of charge from The Cambridge Crystallographic Data Centre via www.ccdc.cam.ac.uk/structures. See SI for details.
[42] X. Li, D. P. Curran, *J. Am. Chem. Soc*. **2013**, *135*, 12076–12081.
[43] D. Drikermann, R. S. Mößel, W. K. Al-Jammal, I. Vilotijevic, *Org. Lett.* **2020**, *22*, 1091–1095.
[44] J.-M. Yang, Y.-T. Zhao, Z.-Q. Li, X.-S. Gu, S.-F. Zhu, Q.-L. Zhou, *ACS Catal.* **2018**, *8*, 7351–7355.
[45] J. Li, H. He, M. Huang, Y. Chen, Y. Luo, K. Yan, Q. Wang, Y. Wu, *Org. Lett.* **2019**, *21*, 9005–9008.
[46] S.-S. Zhang, H. Xie, B. Shu, T. Che, X.-T. Wang, D. Peng, F. Yang, L. Zhang, *Chem. Commun.* **2020**, *56*, 423–426.
[47] J.-M. Yang, F.-K. Guo, Y.-T. Zhao, Q. Zhang, M.-Y. Huang, M.-L. Li, S.-F. Zhu, Q.-L. Zhou, *J. Am. Chem. Soc.* **2020**, *142*, 20924–20929.
[48] M.-Y. Huang, Y.-T. Zhao, H. Chai, C.-D. Zhang, S.-F. Zhu, *CCS Chem.* **2021**, *3*, 1721–1726.
[49] V. Bagutski, T. G. Elford, V. K. Aggarwal, *Angew. Chem. Int. Ed.* **2011**, *50*, 1080−1083; *Angew. Chem.* **2011**, *123*, 1112–1115.
[50] R. Dallanegra, A. B. Chaplin, A. S. Weller, *Angew. Chem. Int. Ed.* **2009**, *48*, 6875–6878; *Angew. Chem.* **2009**, *121*, 7007–7010
[51] C. Werlé, R. Goddard, P. Philipps, C. Farès, A. Fürstner, *J. Am. Chem. Soc.* **2016**, *138*, 3797–3805.

10.1002/anie.202109447

Entry for the Table of Contents

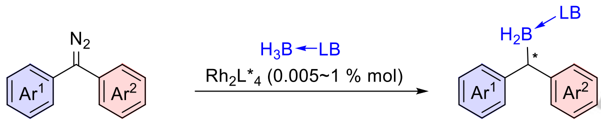

LB = Lewis base

Tolerated functional groups: Cl, Br, F, CF_3, OMe, NO_2, CN, CO_2Me, $CONMe_2$, acetal, SO_2Me, etc.

Tolerated heteroaromatics: indole, benzopyran, pyridine

TON up to 14300

up to 99% yield

up to 99% ee